ELSEVIER

Structural basis of p21$^{H\text{-}ras}$ molecular switch inhibition by a neutralizing antibody

William M. Gallagher* and Guy H. Grant

Department of Biochemistry, University College Dublin, Belfield, Dublin 4, Republic of Ireland

The ras *oncogene product p21 functions as a molecular switch in the early section of the signal transduction pathway that is involved in cell growth and differentiation. When the protein is in its GTP-complexed form it is active in signal transduction, whereas it is inactive in its GDP-complexed form. The transforming activity of p21^{ras} is neutralized by the mouse monoclonal antibody Y13-259, possibly by preventing GDP–GTP exchange. A molecular model of the variable fragment of Y13–259 has been derived using a knowledge-based prediction approach and computer-assisted modeling techniques. An analysis of this model while complexed with p21^{ras}/(GDP) indicated that the two molecular switch regions are constrained by complex formation. Antibody binding inhibits GDP–GTP exchange through a mechanism of steric hindrance. Having identified necessary bound sites for inhibition, and explored their electrostatic properties, it should be possible to proceed with the design of antibody mimics as therapeutic agents in cancer control.*

Keywords: Homology modeling, oncoprotein, molecular switch, monoclonal antibody, anti-cancer drug design

INTRODUCTION

The *ras* family of protooncogenes, which is highly conserved in eukaryotes, is of particular interest because the genes have been implicated in the development of numerous tumors. Three different genes found in the human genome, named (Ha(rvey)-, Ki(rsten)-, and N(euroblastoma)-*ras*, encode 21-kDa proteins that are believed to function as molecular switches in signaling events of cell growth and differentiation.[1] The p21^{ras} proteins, like the G proteins, bind magnesium complexes of guanine nucleotides with high affinities and remarkable selectivity. When bound to GTP they are in their "on" or active state; their GDP complexes comprise the "off" or inactive form. In addition to binding guanine nucleotides, the p21^{ras} proteins exhibit an intrinsic GTPase activity.[2]

Oncogenic forms of p21^{ras} proteins are thought to be in an irreversibly activated state due to inhibition of GTPase activity. Whereas the presence of oncogenic proteins is sufficient for transformation of certain cell lines, high expression of the normal Ras proteins can itself induce morphological transformation. The oncogenic forms of these proteins have amino acid substitutions at any of five specific amino acid positions: 12, 13, 59, 61, and 63.[3] Because these mutations are in the regions of p21^{ras} thought to be involved in guanine nucleotide binding, it was predicted that these mutations would induce transformation as a consequence of a major reduction in intrinsic GTPase activity.

This prediction was questioned because *in vitro* the activating mutations induced only small reductions in GTPase activity. The explanation of this apparent paradox came with the discovery of GTPase-activating protein (GAP). GTPase-activating protein was found to increase the GTPase activity of normal N-Ras more than 200-fold *in vitro* but has no effect on mutant proteins.[4] Mutation studies have identified the sequence 30–40 as the region of GAP binding.[5] Two models for the function of GAP in the mechanism of action of p21^{ras} have been proposed. In the first model, GAP is a p21^{ras}-activated effector protein; in the second, GAP regulates the function of the p21 protein by stimulating its GTPase activity and promoting the generation of the "inactive" GDP-bound form.[6]

It has been suggested that the GTPase hydrolysis reaction triggers a conformational change within p21^{ras} that is a necessary event in the signal transduction pathway.[1] Using X-ray crystallography, several groups have attempted to de-

Color Plates for this article are on page 28 and 29.

Address reprint requests to Dr. Grant at the Department of Chemistry, University College Dublin, Belfield, Dublin 4, Republic of Ireland.
*Present address: CRC Department of Medical Oncology, Alexander Stone Building, Garscube Estate, Switchback Road, Bearsden, Glasgow G61 1BD, Scotland.

Received 2 May 1995; revised 18 January 1996; accepted 23 January 1996.

655 Avenue of the Americas, New York, NY 10010

0263-7855/96/$15.00
PII S0263-7855(96)00020-3

duce the structural differences between the "active" and "inactive" forms of $p21^{ras}$ protein when complexed with guanine nucleotide analogs. From a selection of eight crystal structures, Milburn et al.[7] distinguished between conformational anomalies resulting from (1) differences in crystal packing, and (2) the functional differences induced by the presence of the γ-phosphate in the GTP complex.

These results reveal that the two states of the switch are distinguished by conformational differences that span more than 40 Å and are induced by the γ-phosphate. The most significant differences are localized in two regions; residues 30 to 38 (the switch I region) and residues 60 to 76 (the switch II region). It is proposed that conformational changes in these two regions are necessary for GDP–GTP exchange.

Monoclonal antibody Y13–259 broadly reacts with Ras proteins, including all three mammalian Ras proteins, RAS1 and RAS2 of *Saccharomyces cerevisiae*, and the Ras of *Dictyostelium*. The neutralizing action of Y13–259 has been determined at the biochemical level in its inhibition of Ras stimulation of yeast adenylate cyclase.[8] The epitope for the neutralizing antibody has been identified as the region of residues 63 to 73.[8] This epitope covers most of the switch II region, which has a different conformation in the GDP and the GTP complexes.

It has been demonstrated that Y13–259 severely hampers the nucleotide exchange reaction between p21-bound and exogenous nucleotides but does not interfere with the association of GDP to p21.[9] Therefore, a simple explanation for the neutralizing effect of the antibody would be that antibody binding to Ras proteins would freeze the conformation of the switch II region and prevent GDP–GTP exchange (which requires a conformational change of the region), thus neutralizing the transforming activity of oncogenic Ras proteins.

Structure–function studies have provided a number of approaches in the search for an anti-Ras drug.[3] The observation that Y13–259 binding inhibits GDP–GTP exchange may be utilized in the reduction of the level of activated Ras proteins. However, the antibody shows no specificity for either protooncogenic or oncogenic forms. Such specificity may be engineered into hybrid antibody structures as previously described.[10,11]

This article reports the modeling of the variable fragment (Fv) of the monoclonal antibody Y13–259 and its resultant complex with $p21^{ras}$, which will be of use in understanding specific antibody–antigen interactions. A structural explanation for the neutralizing activity of the antibody has also been obtained. This information may be used in the knowledge-based design of modified antibodies or antibody-loop mimics as therapeutic anticancer agents.

MATERIALS AND METHODS

Construction of the variable fragment model

The amino acid sequences of the Y13–259 variable heavy and light domains (V_H and V_L) were previously determined by cloning experiments.[12] Coordinates of the crystal structures and amino acid sequences of selected immunoglobulins were obtained from the Protein Data Bank[13] as indicated in Table 1. Sequence alignments between the selected immunoglobulins and the experimental sequence were achieved using the Macintosh computer application program, MacMolly.[14] The program aligns sequences automatically using a dynamic programming algorithm.[15] To aid in the determination of the hypervariable loop conformations, the "canonical structure" model devised by Chothia and Lesk[16] was used. Superpositions were accomplished manually using the modeling package *Insight II*[17] as were side-chain substitutions. This work was carried out on a Silicon Graphics Indigo workstation.

Table 1. Sequence homology results: Known immunoglobulin structures versus Y13–259 V_L and V_H

		Similarity (%)[b]	
Immunoglobulin[a]	Origin	Y13–259 V_L	Y13–259 V_H
ANO2	Mouse	59.82	48.06
D1.3	Mouse	**72.32**[c]	52.42
YS*T9.1	Mouse	65.14	58.40
R19.9	Mouse	63.96	52.38
J539	Mouse	57.52	**62.90**[c]
HyHEL-5	Mouse	59.26	52.46
McPC603	Mouse	58.41	59.84
HyHEL-10	Mouse	58.04	47.73
4-4-20	Mouse	55.36	60.48
36-71	Mouse	63.72	54.10
KOL	Mouse	45.61	61.72

[a]The immunoglobulin structures are referred to by their PDB codes.
[b]Sequence alignments were achieved using MacMolly.[14]
[c]Numbers in boldface indicate the most homologous variable domains.

Minimization of the variable fragment

The simulation program CHARMM[18] was used with the united-atom force field to apply dynamics and energy minimization refinement to the substituted structure. First, the molecule was solvated in a 10-Å shell of TIP3P water. Prior to dynamics, minimization was carried out in three steps: (1) minimization of hydrogen atoms to correct stereochemistry (200 steps) with all other atoms constrained, (2) minimization to convergence of side chains with backbone constrained, and (3) minimization to convergence of entire molecule with no constraints. Dynamics was subsequently accomplished by heating to 300 K, followed by equilibration for 10 and 25 psec of free dynamics. Following free dynamics, the structure was cooled to 0 K over 1 psec and minimized to convergence without constraints.

Generation of the antibody–antigen complex

The amino acid sequence and coordinates of the crystal structure of $p21^{H\text{-}ras}$ complexed with GDP was obtained from the Protein Data Bank (PDB code 4Q21).[19] All protein charges were taken from the AMBER charge templates provided with the DelPhi program.[20] GDP charges were obtained using the AM1 Hamiltonian and the ESP method as implemented in MOPAC 6.0.[21] Electrostatic potential grids were created using DelPhi.[20] Solvent-accessible surfaces were calculated using the program MS[22] with a 1.7-Å probe radius. The complex was constructed by interactive manipu-

lation of Connolly surface representations of the two proteins, taking as guidance the experimentally determined epitope regions. Z-clipping of trial structures allowed the complex to be viewed in cross-section, thus avoiding undue van der Waals clashes. Electrostatic potential maps[20] were used to verify the complementarity of the interacting surfaces within the complex.

Refinement of the antibody–antigen complex

The complex was refined in solution using a protocol similar to that applied to the Fv fragment.

Calculation of binding energy

A semiquantitative estimate of the Gibbs free energy change (ΔG) that accompanies the noncovalent complex formation of the Y13–259 Fv fragment with $p21^{ras}$ was calculated according to a previous method.[23] The empirical ΔG function used implicitly incorporates solvent effects and has the following components: hydrophobic force, solvent-modified electrostatics, changes in side-chain conformational entropy, translational/overall rotational entropy changes, and the dilutional (cratic) entropy term. Even using crystal structure data such a procedure cannot be considered as quantitative; however, the calculated ΔG value is likely to be a better indicator of the stability of the complex than the molecular mechanics potential.

RESULTS AND DISCUSSION

Homology and modeling

As only the sequence for the Y13–259 Fv is known, it was modeled on the basis of homology with immunoglobulins of known structure. Comparisons of the known immunoglobulin structures have revealed that their framework regions are similar. Thus, homologous immunoglobulins should have similar framework structures. The amino acid sequences of the Y13–259 V_L and V_H domains were compared with the primary sequences of 11 selected mouse immunoglobulin structures obtained from the Protein Data Bank.[13] Mouse immunoglobulin structures were chosen for sequence comparison so as to limit the homology search to members within the same species.

Table 1 details the results of the sequence alignments. The best match for the Y13–259 V_L was that of the murine anti-lysozyme antibody D1.3,[24] where there was 72.3% amino acid identity, with 7 of the 21 nonidentical residues being conservative replacements. The most similar V_H was the murine galactan-binding immunoglobulin J539,[25] with 62.9% identity and conservative replacements accounting for 18 of the remaining 47 residues. Thus, the V_L of D1.3 and the V_H of J539 were used as framework domains in the construction of the model.

Figure 1 illustrates diagrammatically the resulting amino acid sequence comparisons that were produced using the computer application program MacMolly.[14] It may be seen within the complementarity determining regions (CDR) that the sequences are generally unconserved as would be expected due to their variant nature. Outside the hypervariable regions, the majority of residues are conserved.

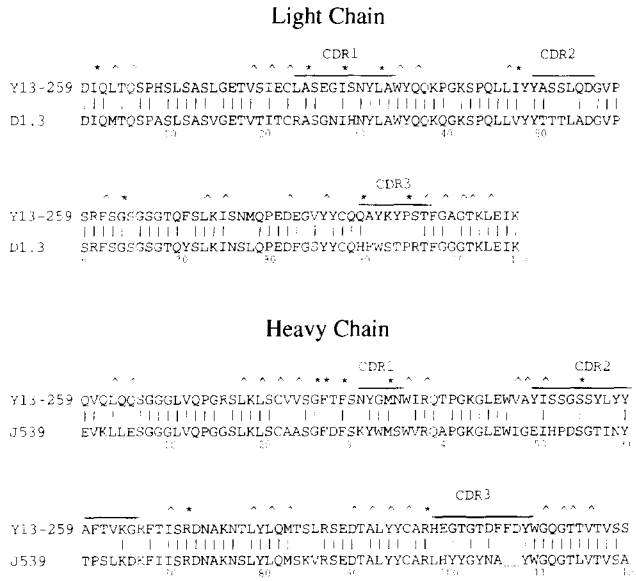

Figure 1. Amino acid sequence comparisons between the template V_L (D1.3) and V_H (J539) and the target structure (Y13–259 Fv). Sequence identity is indicated by a vertical line, differences by a space, and deletions by a dash. Residues buried on V_L:V_H association[5,19] are indicated by a caret, and the conserved residues that are the structural determinants of CDR loop canonical structure[27] are indicated by an asterisk. The residues are numbered according to the Y13–259 Fv sequence. The numbering scheme may be converted to the Kabat[38] scheme, as follows: V_L 1–107; V_H 1–52, 52a, 53–82, 82abc, 83–100, 100abc, 101–113.

This conservation in sequence allows the homologous antibody domains to be used as framework domains in the modeling of the Y13–259 Fv. Therefore, the only difficulties remaining are the modeling of the hypervariable regions and inclusion of the amino acid side chains,. The canonical structures appropriate to the CDRs from the experimental Fv were determined.[16,26,27]

Conformation of the hypervariable regions

In the known V_L structures, the conformations of the L1 regions, residues 26 to 32, are characteristic of the class of the light chain. In V_λ domains their conformation is helical and in the V_κ domains it is extended.[28,29] These conformational differences are attributed to sequence differences in both the L1 region and the framework.[30] The V_L domain of the target is the V_κ class and, thus, by analyzing the conformations of L1 regions in known V_κ domain structures, information on the experimental L1 region was gleaned.

The L1 conformation is determined primarily by the packing of residue 29 against residues 2, 25, 33, and 71 in the interior of the framework. Four different canonical conformations have been observed for L1 hypervariable regions in Vκ domains (Table 2). In Y13–259, L1 has the same length as in HyHEL-10,[31] and the residues packing against the framework are conserved. We predicted L1 of Y13–259 to have the HyHEL-10 conformation (canonical 2). D1.3, although the most homologous V_L as a whole, was not chosen due to a shorter L1 loop.

Table 2. Sequences and conformations of V_κ hypervariable regions of known structure

L1 regions[a]

Canonical[b] structure	Protein	26	27	28	29	30	31	[A–F]	32	2	25	33	71
					*					*	*	*	*
	Y13–259	**S**	**E**	**G**	**I**	**S**	**N**	**—**	**Y**	**I**	**A**	**L**	**F**
2	HyHEL-10	S	Q	S	I	G	N	—	N	I	A	L	F
	D1.3	S	G	N	I	H	N	—	Y	I	A	L	Y
1	J539	S	S	S	V	S	—	—	S	I	A	L	Y
	HyHEL-5	S	S	S	V	S	—	—	Y	I	A	M	Y
3	McPC603	S	E	S	L	L	N	a–f	F	I	S	L	F
4	4-4-20	S	Q	S	L	V	H	a–f, except b	Y	V	S	L	F

L2 regions

Canonical[b] structure	Protein	50	51	51	48	64
					*	*
	Y13–259	**Y**	**A**	**S**	**I**	**G**
1	HyHEL-10	Y	A	S	I	G
	D1.3	Y	T	T	I	G
	McPC603	G	A	S	I	G
	J539	E	I	S	I	G
	HyHEL-5	D	T	S	I	G
	4-4-20	K	V	S	I	G

L3 regions

Canonical[b] structure	Protein	91	92	93	94	95	96	90
						*		*
	Y13–259	**A**	**Y**	**K**	**Y**	**P**	**S**	**Q**
1	HyHEL-10	S	N	S	W	P	Y	Q
	4-4-20	S	T	H	V	P	W	Q
	D1.3	F	W	S	T	P	R	H
	McPC603	D	H	S	Y	P	L	N
					*			*
2	J539	W	T	Y	P	L	I	Q
						*		*
3	HyHEL-5	W	G	R	N	P	—	Q

[a]The residues listed here (single-letter code) are those that form the hypervariable regions and those in the framework regions that are important for the observed conformations of these regions. The hypervariable regions are taken as those outside the β sheet.
[b]The sequences are grouped together so that those that have the same main-chain conformation or canonical structure are adjacent. The canonical structure numbers are used to indicate the different conformations.[27] The residues in the hypervariable and framework regions that are mainly responsible for these conformations are indicated by an asterisk.

Only one main-chain canonical structure for L2 has been detected in the immunoglobulin structures determined to date.[27,32] The similarities in the L2 structures arise from the conformational requirements of a three-residue turn and the conservation of the framework residues against which L2 packs. These three residues link two adjacent strands in the framework β sheet. The side chains of L2 all point toward the surface. The main chain packs against the conserved framework residues Ile-48 and Gly-64. These conserved residues are strong determinants of whether a particular L2 conformation is adopted. The L2 of HyHEL-10 conforms exactly to the sequence of Y13–259 at both the loop and important framework positions. Therefore, HyHEL-10 was chosen as a model for the L2 region of Y13–259.

The L3 region, residues 91 to 96, forms the link between two adjacent strands of β sheet. Analysis of the structures

and sequences known for this region indicated that the majority of κ chains have a common conformation that is quite different from the conformations found in λ chains.[16] Important determinants of the particular L3 conformation found in κ chains are the hydrogen bonds formed to its main-chain atoms by the side chain of framework residue 90, usually glutamine. The presence of Pro-95 disallows hydrogen bonding with residue 92, resulting in an extended four-residue turn characteristic of canonical 1. J539, has a different canonical structure due to the presence of Leu-95 allowing the formation of a two-residue turn (canonical 2). Canonical 3 is formed when L3 is five residues long as in the case of HyHEL-5.

The experimental L3 was six residues long, had proline and glutamine at positions 95 and 90 respectively, which meant that HyHEL-10 and 4-4-20 were the only suitable candidates remaining. HyHEL-10 had greater sequence identity and was chosen as a model for the L3 of Y13–259 once again. NQ10 and NC41 had both good sequence identity with Y13–259 and the required conserved residues, but the antibody structures were not available in the Protein Data Bank and, therefore, could not be used.

The H1 regions are seven residues in length in all known structures found to date.[27] In the observed H1 structures the glycine at position 26 produces a sharp turn through a ϕ, ψ value (+75, 0) outside the range allowed for nonglycine residues. The residue at position 29 tends to be deeply buried within the framework structure, packing against the side chain of residue 34 and the main-chain residues 72 and 77. The residue at position 27 also appears to be an important determinant of H1 conformation as it is commonly buried in a surface cavity next to residue 94.

Most of the structures occupy the canonical 1 conformation, whereas HyHEL-10 has been shown to exist in an alternative form denoted canonical 1′ (Table 3). In Y13–259, H1 also has seven residues and the important side chains predicted its conformation to be that of canonical 1. The H1 structures from McPC603, KOL, and J539 complied exactly with the conserved residue requirements of Y13–259. However, J539 was used in the modeling of the experimental loop as it had the most similar V_H as a whole.

The H2 region forms the link between the framework residues 52 and 56, which are in adjacent strands of β sheet. The H2 loops differ in size and conformation in the known V_H structures.[16] Four canonical conformations have been observed to date for H2 regions (Table 3). Again, certain conserved residues exist that determine the conformation adopted. In Y13–259, H2 has four residues and the presence

Table 3. Sequences and conformations of V_H hypervariable regions of known structure[a]

H1 regions

Canonical structure	Protein	26	27	28	29	30	31	32	34	94
		*	*		*				*	*
	Y13-259	**G**	**F**	**T**	**F**	**S**	**N**	**Y**	**M**	**R**
1	J539	G	F	D	F	S	K	Y	M	R
	McPC603	G	F	T	F	S	D	F	M	R
	KOL	G	F	I	F	S	S	Y	M	R
	D1.3	G	F	S	L	T	G	Y	V	R
	HyHEL-5	G	Y	T	F	S	D	Y	I	R
	4-4-20	G	F	T	F	S	D	Y	M	G
1′	HyHEL-10	G	D	S	I	T	D	D	W	N

H2 regions

Canonical structure	Protein	52a	b	c	53	54	55	71
						*		*
	Y13–259	**S**	—	—	**G**	**S**	**S**	**R**
3	J539	P	—	—	D	S	G	R
	KOL	D	—	—	D	G	S	R
		*					*	*
2	HyHEL-5	P	—	—	G	S	G	A
						*	*	*
4	McPC603	N	K	G	N	K	Y	R
	4-4-20	N	K	P	Y	N	Y	R
							*	
1	D1.3	—	—	—	Y	H	G	
	HyHEL-10	—	—	—	Y	S	G	

[a]The residues are listed in the same format as Table 2.

of Arg-71 indicated the predicted structure to be similar to canonical 3. McPC603 and 4-4-20 (canonical 4) were excluded owing to their excessive length. KOL and J539 differ in conformation depending on the position of glycine or serine at position 54. Y13–259 has a serine at this residue position, and, thus, should correspond more exactly to the H2 of J539. Therefore, the H2 of J539 was used as a model for the experimental H2 loop.

Crystal structures of known H3 loops do not have obvious canonical forms and vary greatly in length and conformation. The H3 region consists of residues 96 to 101. In McPC603, the conformation of H3 is determined mainly by the interactions of residues Arg-94, Tyr-100b, Phe-100c, and Asp-101 within the V_H domain and at the V_L–V_H interface.[16,28] In McPC60,[33] Tyr-100b packs into a large cavity adjacent to Tyr-49 of V_L. The hydroxyl groups of both tyrosine residues are on the surface. Tyrosine or phenylalanine occurs at position 49 in 82% of V_L domains.[16] Different residues at the position equivalent to 100b can produce different H3 conformations. For example, in KOL it is glycine and the cavity adjacent to Tyr-49 in V_L is filled by phenylalanine at a position equivalent to 100a. This contributes to making the conformation of H3 in KOL very different from that found in McPC603. Y13–259 differs from McPC603 at only one residue position, Phe-100b. In J539, the H3 loop was two residues shorter than in Y13–259. Therefore, McPC603 was used in the modeling of the experimental H3 loop.

Overall, it was found that HyHEL-10 had canonical structures for CDRs 1–3 more appropriate to the Y13–259 V_L sequence than D1.3. In the case of Y13–259 V_H, the canonical structure of the McPC603 CDR 3 was more appropriate. The predicted conformations for the other two hypervariable regions of the heavy chain were present in the parent V_H framework structure.

By the above method, appropriate canonical structures for the hypervariable regions of Y13–259 were selected. If the conformation predicted for a region was not present in the parent framework domain, but was present in another known structure, the hypervariable region in the parent was replaced (grafted) by that in the other structure.

The antibody variable fragment model

Once the hypervariable loops were grafted, the V_L and V_H hybrids were then orientated so as to maintain the normal domain associations. It has been shown that among the known immunoglobulin structures determined to date several conserved residues exist that are involved in packing of the variable domains.[34] These residues were present in the structures used for experimentation as illustrated in Fig. 1. A composite Fv domain was created with the V_L of D1.3 and the V_H of J539 in which most of the "key" residues and their interactions in the V_L:V_H interface were conserved. This composite Fv was subjected to modification of the amino acid residues to comply with the primary sequence of Y13–259.

The crude variable fragment model was subjected to energy minimization and molecular dynamics refinement using the CHARMM program.[18] This produced a considerable reduction in the energy of the model structure. Finally, energy minimization of the quenched structure gave an energy of −4495.89 kcal/mol. This can be compared to the starting energy of −3833.00 kcal/mol (a difference of 652.89 kcal/mol). The root mean square (rms) differences were calculated between the starting structure and the fully refined structure (Table 4). The results indicated that the refinement procedure had not completely disrupted the starting structure. The protein backbone of the model is shown in Fig. 2. This α-carbon tracing shows that the general immunoglobulin domain "β-barrel" structure has been maintained.

The antibody–antigen complex

Once the refinement had been completed, the model was used to study possible interactions with $p21^{ras}$/(GDP); it has been hypothesized that the antibody interacts only with this form of the antigen.[7] Solvent-accessible surfaces were calculated for both structures around the probable binding site areas. This allowed the visualization of the shape of the interacting surfaces. The antigen-combining site of the Y13–259 Fv has a relatively deep groove in comparison to the majority of discovered antibody-binding sites.[10] Analysis of the solvent-accessible surface near the epitope of $p21^{ras}$ [8] revealed a considerable projection from the main body of the protein. An obvious similarity existed between the antigen projection and the interdomain groove of the Fv.

The antigen could be placed into the binding site groove in either of two modes, related to one another by an ~180° rotation about the central pocket. In each binding mode, there is steric complementarity between the surfaces of the antigen and the antigen-combining site. Poisson–Boltzmann electrostatic potentials, calculated using the DelPhi program,[20] show that only one of the binding modes allows favorable electrostatic complementarity, which is a necessary facet of complex formation (Color Plate 1). This binding mode was utilized in the docking of the antibody and antigen structures. Once the complex was formed, it was subjected to energy minimization and molecular dynamics using CHARMM.[18]

Antibody–antigen interactions

The extent of the interaction between Y13–259 Fv and $p21^{ras}$ was evaluated by calculating the loss of exposed surface area on the formation of the complex. The minimized complex revealed a buried surface area of 230.3 Å^2 at the antigen-binding site, which is considerably smaller than that of the majority of antibody–antigen complexes, especially those in which the antigen is lysozyme.[10,11] Ap-

Table 4. Root mean square differences between starting and refined structure

Atom selection[a]	rms (Å)
All atoms	2.02
All nonhydrogen atoms	1.77
Backbone atoms	1.33
α-Carbon atoms	1.31

[a]Atom selection refers to the atoms on which the calculation was determined.

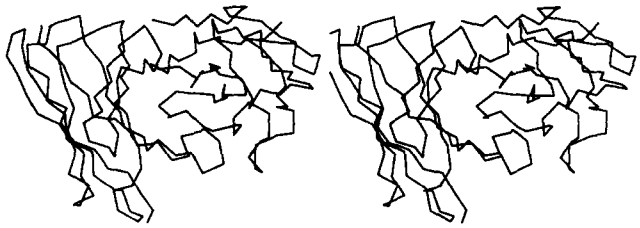

Figure 2. The β-barrel structure of the Y13–259 Fv model. The α-carbon backbone of the Y13–259 Fv model is shown looking down onto the antigen-binding site. Stereo pair images are used.

proximately 4.0% of the antigen surface area becomes buried on association with the antibody. This is slightly lower than the values obtained with other antibody–antigen complexes. The total buried surface area at the antibody–antigen interface is 478.6 Å^2, which is again relatively small.

It has been suggested that the optimal shape of an antigen-combining site for a large ligand, such as a protein, depends mainly on the radius of curvature of the epitope on the antigen.[35] Although p21^{ras} is larger than lysozyme, the projection of the epitope from the main body of the protein may provide an explanation for the apparently small buried surface area. The variable fragment of Y13–259 complements this particular epitope topology by having an interdomain groove characterized by a deep pocket. In contrast, lysozyme epitopes have much flatter surfaces resulting in shallow antigen-combining sites on respective antibodies. Thus, the complex between Y13–259 Fv and p21^{ras} may be considered as a novel type (Color Plate 2).

Approximately 10 CDR residues contribute to the overall buried surface area. A breakdown of the contributions of the light and heavy chain CDRs shows a preferential interaction of the antigen with the heavy chain (Table 5). Although the antigen is bound along the pseudo-two-fold axis relating V_L and V_H, almost two-thirds of the contacts involve the heavy chain. However, only two of the six CDRs, L3 and H2, make contacts with the antigen. Other antigen–antibody complexes also have interactions dominated by the heavy chain[11,36] but this lack of participation in the complex by the majority of CDRs has not been previously observed.

Table 5. Breakdown of CDR buried surface area in complex[a]

Chain	Sequence	Buried surface area (%)
	24 34	
L1	LASEGISNYLA	0
	50 56	
L2	YASSLQD	0
	90 98	
L3	QA**YKYP**STF	41
	31 35	
H1	NYGMN	0
	50 A 65	
H2	**YISSGSSY**L**Y**YAETVK	51
	95 ABC 102	
H3	HEGTGTDFFDY	0

[a]Residues of Y13–259 Fv that are part of the buried surface area are in boldface, and the residues that are the largest contributors to the buried surface area are in underlined boldface. Surface area values were calculated by the program MS[22] using a 1.7-Å probe. The total buried surface area for Y13–259 Fv is 248.3 Å^2 and for p21^{ras} is 230.3 Å^2.

Half of the buried residues in the antibody are aromatic in nature; in fact, they are all tyrosine residues. It has been suggested that amphipathic amino acids, such as tyrosine could readily tolerate the change of environment from hydrophilic to hydrophobic that occurs on antibody–antigen complex formation.[37] Such amino acids having flexible side chains could generate a structurally plastic region. A binding site possessing this ability to mold itself around the antigen would improve complementarity of the interacting surfaces. Most of the remaining buried residues are serines, which have a polar character suggesting possible hydrophilic interactions.

Within the antibody–antigen complex, 17 van der Waals contacts were determined using the contact distance given previously.[24] Only two of the five contract residues of the bound antigen agree with epitope-mapping results from an earlier immunological study.[8] However, all of the antigen contact residues lie within the two molecular switch regions (Table 6). Within the V_H domain, there are five contacts that are close enough to be possible hydrogen bonds; within the V_L domain, there are none.

The most crucial interactions in the complex involve residues from CDR H2. Tyr^{H58} contributes significantly toward hydrophobic and van der Waals interactions with the antigen and also forms two hydrogen bonds to Glu-63^{Ras}. Two serine residues, Ser^{H52} and Ser^{H55}, form polar contacts with Glu-63^{Ras} and Glu-37^{Ras}, respectively. Important hydrophobic and van der Waals interactions occur in the complex due to Tyr^{L94}.

DETERMINATION OF BINDING ENERGY

In general, two macromolecules in solution must overcome large entropic barriers before they can form a tight association. There is the loss of entropy of free rotation and translation of the separate molecules, and there is a loss of conformational entropy of mobile segments and of side chain

Table 6. Antibody Y13–259 Fv residues in contact with P21^{ras}

	Antibody	Antigen[a]
Light chain		
CDR1		
CDR2		
CDR3	Tyr-94	Ala-66
Heavy chain		
CDR1		
CDR2	Ser-52	Glu-63
	Ser-55	Thr-35, Glu-37
	Tyr-56	Thr-35, Glu-37, Glu-63
	Tyr-58	Glu-37, Glu-63, Arg-68
CDR3		

[a]Residues involved in molecular switch mechanism: switch I (30–38), switch II (60–77).

on binding.[11] On the other hand, entropy is gained when water molecules are displaced from the surfaces that become the interface. This latter effect is significant and it appears that water molecules are almost totally excluded from the interface by the close shape complementarity of the surfaces. Enthalpic contributions arise from van der Waals interactions together with the more specific hydrogen bonds and salt bridges.

Using the method of Novotny et al.,[23] we calculated the Gibbs free energy of Y13–259 Fv/p21^{ras} complex formation to be −5.3 kcal/mol and the affinity to be on the order of 130 μmol. These values are consistent with other antibody–antigen complexes.[11,23]

CONCLUSIONS

A molecular model of the Y13–259 Fv/p21^{ras} complex has now been described. The mode of antibody–antigen interaction exhibited in this model is of a novel type. Although p21^{ras} is a relatively large antigen the buried surface area it contributes to the complex is relatively small. The main cause is that the epitope projects sharply from the globular portion of the protein, unlike some other antibody–protein complexes. Another novel feature of the complex is the sole contribution of only one CDR from each chain to antibody–antigen interaction. Overall, it appears that Y13–259 Fv makes very specific contacts with p21^{ras} to exert its biological function.

Using this model, it was found that the antibody interacts specifically with the two molecular switch regions within the antigen. This information suggests that Y13–259 neutralizes the transforming activity of p21^{ras} by conformationally restraining the switch regions so that GTP–GDP exchange is unable to occur (Color Plate 2). Therefore, a structural basis for the neutralizing activity of the antibody against the antigen has been obtained.

This information may be utilized in the reduction of the level of activated Ras proteins. The antibody exhibits no specificity for either normal or mutated forms of p21^{ras}. It is possible that such specificity may be engineered into hybrid antibody structures. For example, the residues on CDR^{L3} and CDR^{H2} are ideal for modification because these loops are close in proximity to the combining site. Knowledge-based substitution of specific residues could enhance binding of the antibody to oncogenic forms of the Ras protein. Modified antibodies or antibody-loop mimics could be used as therapeutic anticancer agents.

ACKNOWLEDGMENTS

The authors thank Biosym Technologies Ltd. for the provision of software under the University Grants Scheme and St. Luke's Institute of Cancer Research for a generous allocation of computer time.

REFERENCES

1 Wittinghofer, A., and Pai, E.F. The structure of *ras* protein: A model for a universal molecular switch. *Trends Biochem. Sci.* 1991, **16,** 382–387

2 Gibbs, J.B., Sigal, I.S., and Scholnick, E.M. Biochemical properties of normal and oncogenic *ras* p21. *Trends Biochem. Sci.* 1985, **10,** 350–353

3 Sigal, I.S., Smith, G.M., Jurnak, F., Marsico-Ahern, J.D., D'Alonzo, J.S., Scolnick, E.M., and Gibbs, J.B. Molecular approaches towards an anti-*ras* drug. *Anti-Cancer Drug Design* 1987, **2,** 107–115

4 Wakelam, M.J.O., Black, F.M., and Davies, S.A. The role of *ras* gene products in second messenger generation. *Biochem. Soc. Symp.* 1989, **56,** 103–116

5 Aldari, H., Lowry, D.R., Willumsen, B.M., Der, C.J., and McCormick, F. Guanosine triphosphatase activating protein (GAP) interacts with the p21^{ras} effector binding domain. *Science* 1988, **240,** 518–521

6 Bourne, H.R., Sanders, D.A., and McCormick, F. The GTPase superfamily: Conserved structure and molecular mechanism. *Nature (London)* 1991, **349,** 117–127

7 Milburn, M.V., Tong, L., De Vos, A.M., Brunger, A., Yamaizumi, Z., Nishimura, S., and Kim, S.-H. Molecular switch for signal transduction: Structural differences between active and inactive forms of protooncogenic *ras* proteins. *Science* 1990, **247,** 939–945

8 Sigal, I.S., Gibbs, J.B., D'Alonzo, J.S., and Scolnick, E.M. Identification of effector residues and a neutralizing epitope of Ha-*ras*-encoded p21. *Proc. Natl. Acad. Sci. U.S.A.* 1986, **83,** 4725–4729

9 Hattori, S., Clanton D.J., Satoh, T.A., Nakamura, S., Kaziro, Y., Kawakita, M., and Shih, T.Y. Neutralizing monoclonal antibody against *ras* oncogene product p21 which impairs guanine nucleotide exchange. *Mol. Cell. Biol.* 1987, **7,** 1999–2002

10 Wilson, I.A., and Stanfield, R.L. Antibody-antigen interactions. *Curr. Opin. Struct. Biol.* 1993, **3,** 113–118

11 Davies, D.R., Padlan, E.A., and Sheriff, S. Antibody–antigen complexes. *Annu. Rev. Biochem.* 1990, **59,** 439–473

12 Werge, T.M., Biocca, S., and Cattaneo, A. Intracellular immunization. Cloning and intracellular expression of a monoclonal antibody to the p21^{ras} protein. *FEBS Lett.* 1990, **274,** 193–198

13 Bernstein, F.C., Koetzle, T.F., Williams, G.J.B., Meyer, E.F., Jr., Brice, M.D., Rogers, J.R., Kennard, O., Shimanouchi, T., and Tasumi, M. The Protein Data Bank: A computer-based archival file for macromolecular structures. *J. Mol. Biol.* 1977, **112,** 535–542

14 Soft Gene. *MacMolly,* version 3.5.3. Soft Gene GmbH, Heidelberg, Germany

15 Needleman, S.B., and Wunsch, C.D. A general method applicable to the search for similarities in the amino acid sequence of two proteins. *J. Mol. Biol.* 1970, **48,** 443–453

16 Chothia, C., and Lesk, A.M. Canonical structures for the hypervariable regions of immunoglobulins. *J. Mol. Biol.* 1987, **196,** 901–917

17 Biosym Technologies. *Insight II User Guide,* version 2.2.0. Biosym Technologies, San Diego, California, 1993

18 Brooks, B.R., Bruccoleri, R.E., Olafson, B.D., States, D.J., Swaminathan, S., and Karplus, M. CHARMM: A program for macromolecular energy, minimisation and dynamics calculations. *J. Comput. Chem.* 1983, **4,** 187–217

19 Tong, L., de Vos, A.M., Milburn, M.V., and Kim, S.H. Crystal structures at 2.2 Å resolution of the catalytic domains of the normal Ras protein and an oncogenic mutant complexed with GDP. *J. Mol. Biol.* 1991, **217,** 503–516

20 Sharp, K.A., and Honig B. (1990). Electrostatic interactions in macromolecules: Theory and applications. *Annu. Rev. Biophys. Biophys. Chem.* **19,** 301–332

21 Dewar, M.J.S, Zoebisch, E.G., Healy, E.F., and Stewart, J.J.P. AM1: A new general purpose quantum mechanical molecular model. *J. Am. Chem. Soc.* 1985, **107,** 3902–3909

22 Connolly, M.L. Analytical molecular surface calculation. *J. Appl. Crystallogr.* 1987, **16,** 548–558

23 Novotny, J., Bruccoleri, R.E., and Saul, F.E. On the attribution of binding energy in antigen–antibody complexes McPC603, D1.3, and HyHEL-5. *Biochemistry* 1989, **28,** 4735–4749

24 Fischmann, T.O., Bentley, G.A., Bhat, T.N., Boulot, G., Mariuzza, R.A., Phillips, S.E.V., Tello, D., and Poljak, R.J. Crystallographic refinement of the three-dimensional structure of the FabD1.3-lysozyme complex at 2.5 Å resolution. *J. Biol. Chem.* 1991, **266,** 12915–12920

25 Suh, S.W., Bhat, T.N., Naria, M.A., Cohen, G.H., Rao, D.N., Rudikoff, S., and Davies, D.R. The galactan-binding immunoglobulin Fab-J539. An X-ray diffraction study at 2.6 Å resolution. *Proteins* 1986, **1,** 74–80

26 Chothia, C., Lesk, A.M., Levitt, M., Amit, A.G., Mariuzza, R.A., Phillips, S.E.V., and Poljak, R.J. The predicted structure of immunoglobulin D1.3 and its comparison with the crystal structure. *Science* 1986, **233,** 755–758

27 Chothia C., Lesk, A.M., Tramontano, A., Levitt, M., Smith-Gill, S.J., Air, G., Sheriff, S., Padlan, E.A., Davies, D., Tulip, W.R., Colman, P.M., Spinelli, S., Alzari, P.M., and Poljak, R.J. Conformations of immunoglobulin hypervariable regions. *Nature* (*London*) 1989, **343,** 877–883

28 Padlan, E.A., Davies, D.R., Pecht, I., Givol, D., and Wright, C. Model-building studies of antigen-binding sites. Hapten binding of MOPC-315. *Cold Spring Harbor Symp. Quant. Biol.* 1977, **41,** 627–637

29 de la Paz, P., Sutton, B.J., Darsley, M.J., and Rees, A.R. Modeling of the combining site of three anti-lysozyme monoclonal antibodies and of the complex between one of the antibodies and its epitope. *EMBO J.* 1986, **5,** 415–425

30 Lesk, A.M., and Chothia, C. Evolution of proteins formed by β-sheets. II. The core of the immunoglobulin domains. *J. Mol. Biol.* 1982, **160,** 325–342

31 Padlan, E.A., Silverton, E.W., Sheriff, S., Cohen, G.H., Smith-Gill, S.J., and Davies, D.R. Structure of an antibody–antigen complex. Crystal structure of the HyHEL-10 Fab–lysozyme complex. *Proc. Natl. Acad. Sci. U.S.A.* 1989, **86,** 5938–5942

32 Barré, S., Greenberg, A.S., Flajnik, M.F. and Chothia, C. Structural conservation of hypervariable regions in immunoglobulin evolution. *Nature Struct. Biol.* 1994, **1,** 915–920

33 Satow, Y., Cohen, G.H., Padlan, E.A., and Davies, D.R. Phosphocholine binding immunoglobulin Fab McPC603: An X-ray diffraction study at 2.7 Å. *J. Mol. Biol.* 1986, **190,** 593–604

34 Chothia, C., Novotny, J., Bruccoleri, B., and Karplus, M. Domain association in immunoglobulin molecules. The packing of variable domains. *J. Mol. Biol.* 1985, **186,** 651–663

35 Tulip, W.R., Varghese, J.N., Laver, W.G., Webster, R.G., and Colman, P.M. Refined crystal structure of the influenza virus N9 neuraminidase–NC41 Fab complex. *J. Mol. Biol.* 1992, **227,** 122–148

36 Garcia, K.C., Ronco, P.M., Verroust, P.J., Brünger, A.T., and Amzel, L.M. Three-dimensional structure of an angiotensin II-Fab complex at 3 Å: Hormone recognition by an anti-idiotypic antibody. *Science* 1992, **257,** 502–507

37 Mian, S.I., Bradwell, A.R., and Olson, A.J. Structure, function and properties of antibody binding sites. *J. Mol. Biol.* 1991, **217,** 133–151

38 Kabat, E.A., Wu, T.T., Reid-Miller, M., Perry, H.M., and Gottesman, K.S. *Sequences of Proteins of Immunological Interest* 4th Ed. National Institute of Health, Bethesda, Maryland, 1987